

**Biolayer Interferometry provides a robust method for detecting DNA-binding small molecules in microbial extracts**

Ross D. Overacker, Birte Plitzko, Sandra Loesgen<sup>‡,\*</sup>

Department of Chemistry, Oregon State University, Corvallis, OR 97331, USA.

<sup>‡</sup> Current Address: Whitney Laboratory for Marine Bioscience, Department of Chemistry, University of Florida, St. Augustine, Florida 32080, United States.

E-mail: [sandra.loesgen@whitney.ufl.edu](mailto:sandra.loesgen@whitney.ufl.edu)

**KEYWORDS:** DNA intercalation, DNA groove binding, Biolayer Interferometry, Microbial natural products

## Abstract

DNA replication is an exceptional point of therapeutic intervention for many cancer types and several small molecules targeting DNA have been developed into clinically used antitumor agents. Many of these molecules are naturally occurring metabolites from plants and microorganisms, such as the widely used chemotherapeutic doxorubicin. While natural product sources contain a vast number of DNA binding small molecules, isolating and identifying these molecules is challenging. Typical screening campaigns utilize time-consuming bioactivity-guided fractionation approaches, which use sequential rounds of cell-based assays to guide the isolation of active compounds. In this study, we explore the use of Biolayer Interferometry (BLI) as a tool for rapidly screening natural products sources for DNA targeting small molecules. We first verified that BLI robustly detected DNA binding using designed GC and AT rich DNA oligonucleotides with known DNA intercalating, groove-, and covalent-binding agents including actinomycin D (**1**), doxorubicin (**2**), ethidium bromide (**3**), propidium iodide (**4**), Hoechst 33342 (**5**), netropsin (**6**), and cisplatin (**7**). Although binding varied with the properties of the oligonucleotides, measured binding affinities agreed with previously reported values. We next utilized BLI to screen over 100 bacterial extracts from our microbial library for DNA binding activity and found three highly active extracts. Binding-guided isolation was used to isolate the active principle component from each extract, which were identified as echinomycin (**8**), actinomycin V (**9**), and chartreusin (**10**). This biosensor-based DNA binding screen is a novel, low cost, easy to use, and sensitive approach for medium-throughput screening of complex chemical libraries.

DNA targeting drugs are known to show significant antibacterial<sup>1</sup>, antiviral<sup>2</sup>, and anticancer bioactivities.<sup>3</sup> In particular, DNA binding chemotherapeutic agents take advantage of the fact that cancer cells are highly prone to DNA damage due to their lenient DNA repair capabilities and increased propagation resulting from their ability to bypass certain cell-cycle checkpoints.<sup>4,5</sup> The first DNA binding chemotherapeutics were developed in the 1950s from anthracyclines isolated from a culture of *Streptomyces purpurascens*.<sup>6</sup> Originally, anthracyclines were pursued as antibiotics, but abandoned when their high toxicity in mice models prevented their antimicrobial application.<sup>7</sup> Instead, the anthracycline doxorubicin was approved in 1976 as a potent antitumor agent that targets DNA via base-pair intercalation. Subsequent searches have identified additional DNA binding agents, such as cisplatin, antimetabolites like 5-fluorouracil, or the topoisomerase poison etoposide, which targets protein-DNA complexes.<sup>4</sup> Anticancer drugs that target DNA can cause changes in DNA confirmation through either intercalation, groove binding, or covalent attachment. These binding events typically result in inhibition of duplication or transcription through DNA strand breakage that can lead to cell death.<sup>8</sup> Despite their inherent non-selectivity, DNA binding drugs such as the anthracyclines (e.g. doxorubicin and daunorubicin) remain indispensable instruments in anticancer therapy today.<sup>9</sup> For example, 32% of breast cancer patients, 57-70% of elderly lymphoma patients, and 50-60% of childhood cancer patients use anthracyclines as the treatment of choice due to their therapeutic effectiveness and low rate of tumor resistance.<sup>10</sup> Even with advances in chemotherapy, cancer diagnoses and deaths have continued to grow, culminating in 1,735,350 new cases of cancer diagnosed in 2018 in the United States alone.<sup>11</sup> A multifaceted approach is needed to combat cancer and emerging chemoresistance. Besides more selective cell targeting and immunotherapy approaches,<sup>12</sup> new

molecules that induce damage to DNA through indirect or direct binding events are needed to serve as drug leads or molecular probes in ongoing research.<sup>13</sup>

Identifying novel compounds that specifically target DNA has historically been challenging due to DNA's extreme flexibility, an absence of 'typical' binding sites as seen in many proteins, and its limited ability to reveal spatial information from X-ray crystallization or nuclear magnetic resonance (NMR).<sup>3</sup> Additionally, DNA binding affinities, thermodynamic signatures, and selectivity vary largely for different binding modes.<sup>14</sup> For example, DNA intercalating agents are relatively flat molecules able to insert themselves between base pairs resulting in lengthening, stiffening, and/or unwinding of helical DNA.<sup>8</sup> These binding events cause significant changes in the structure of DNA that can be detected by many analytical techniques including mass spectrometry (MS)<sup>15-17</sup>, NMR<sup>18</sup>, isothermal calorimetry (ITC)<sup>14,19</sup>, UV absorption spectroscopy<sup>20</sup>, light scattering<sup>21</sup>, fluorescent displacement<sup>22</sup>, and surface plasmon resonance (SPR).<sup>23</sup> On the other hand, minor groove binding agents such as netropsin (**6**), which fit into the small groove of DNA, cause only small perturbations to the overall DNA structure which can be difficult to detect using current methods.<sup>24</sup> The bio-physical techniques used to identify DNA-drug binding and the associated binding affinity vary from laboratory to laboratory, the same is true for the DNA used in these experiments. Most DNA binding screens are time intensive, often costly, and generally not sufficiently sensitive or robust enough for analysis of complex mixtures (e.g. natural extracts for the purpose of drug discovery).<sup>25</sup> Popular techniques such as ITC generally require large quantities of analytes and are sensitive to changes in buffer, temperature, and pH, which limits its application to screen libraries of complex samples.<sup>26</sup> Similarly, SPR has modest screening throughput and its microfluidics design presents challenges for complex samples like microbial or plant derived extracts. Specifically, solubility issues may arise when the samples are flushed

around the sensor chips and unspecific binding to the complex chip matrix has been observed.<sup>27</sup> Changes in analyte preparation including the buffers used can induce variations in the refractive index being measured.<sup>28</sup> In our search for a robust and comparative method to assess DNA binding of small molecules and to screen for DNA interactions within complex mixtures, we developed a low cost, reusable, and medium-throughput method utilizing Biolayer Interferometry (BLI).

BLI allows for the real-time detection of biomolecular binding events between an immobilized ligand and analytes by utilizing disposable optical fiber sensors. This system monitors the spectrum of light reflected off the surface, which varies with binding as a result of minute changes in the optical thickness and corresponding shifts in the optical interference pattern.<sup>25</sup> While BLI has typically been used for studying the binding kinetics of macromolecules such as protein-protein<sup>29</sup> or protein-DNA/RNA<sup>30,31</sup> binding events, it has also been shown to be an excellent screening tool for small molecule interactions.<sup>27,32,33</sup> Here, we show for the first time that BLI is a suitable tool for the reliable and efficient detection of DNA/small molecule binding events within complex microbial extracts. Additionally, we found that BLI serves as a suitable method in determining comparable affinity values to many well-known small molecules. First, we designed model duplex DNA and used it to validate the binding affinities of well-known DNA intercalating and groove binding agents (**Figure 1**). This approach allowed us to define binding affinities for six commonly used DNA-acting agents, including actinomycin D (**1**), doxorubicin (**2**), ethidium bromide (**3**), propidium iodide (**4**), Hoechst 33342 (**5**), netropsin (**6**), and cisplatin (**7**) under highly reproducible conditions. We then compared these results to previously reported binding affinities in the literature. Next, we used BLI to identify DNA binding agents from our microbial natural product extract library containing over 100 bacterial extracts by following the workflow depicted in **Figure 2**. We employed binding-guided isolation paired with HPLC separation to identify and

purify DNA acting compounds. For each metabolite, we determined its binding kinetics against both GC and AT rich DNA.

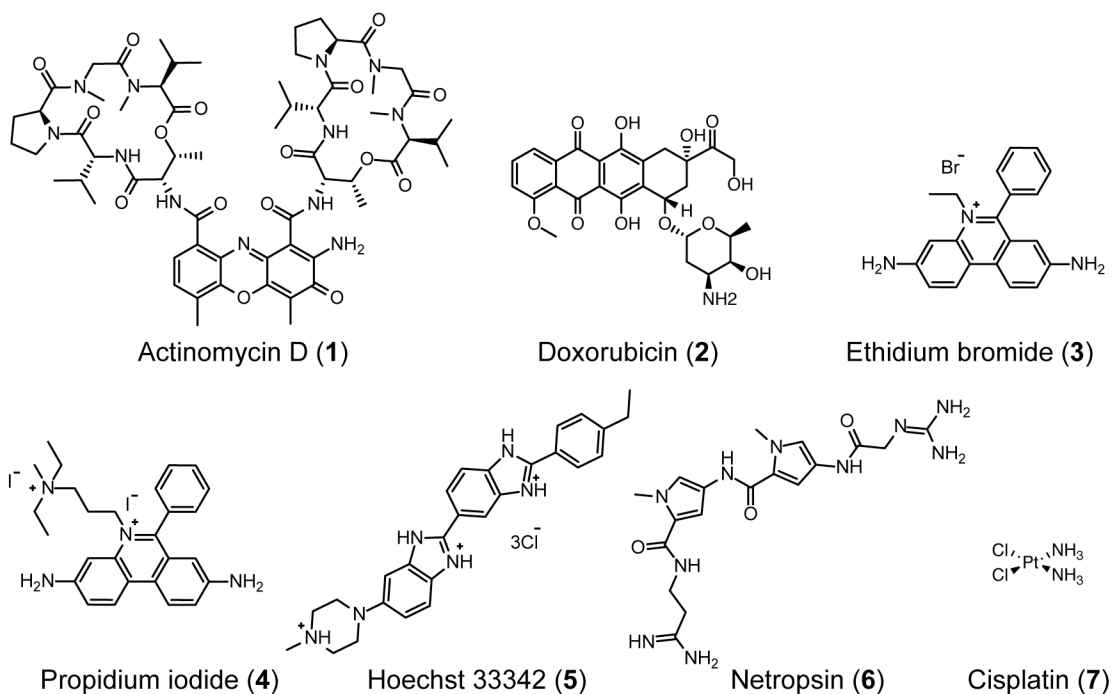


**Figure 1:** A selection of commercially available DNA binding agents used in this study, including DNA intercalating (1, 2, 3, 4), groove binding (5, 6), and covalent binding agents (7).

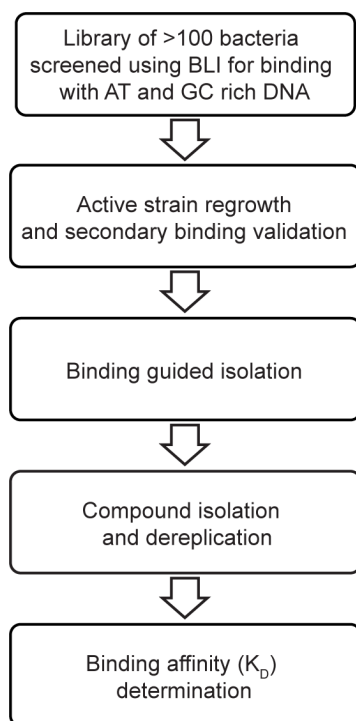


**Figure 2:** Workflow to screen for DNA binding natural products. Extracts were screened for binding at 100  $\mu\text{g}/\text{mL}$ . Binding-guided isolation was used to isolate compounds and their binding affinities to both GC and AT rich DNA oligonucleotides was determined.

## Experimental Section

### Materials and Reagents

Actinomycin D (**1**) was purchased from AdooQ Bioscience (Irvine, CA). Doxorubicin (**2**) was purchased from ThermoFisher Scientific (Waltham, MA). Ethidium bromide (**3**), propidium iodide (**4**), Hoechst 33342 (**5**), netropsin (**6**), and cisplatin (**7**) were purchased from VWR (Radnor, PA). All compounds used were tested for purity prior to use by LCMS. Streptavidin biosensors and Kinetics Buffer (1x PBS, pH 7.4, 0.02% Tween-20, 0.1% albumin, and 0.05% sodium azide) were purchased directly from Molecular Devices (San Jose, CA). Solvents and culture media components were all purchased from VWR unless otherwise noted.

## General experimental procedures

Low- and high-resolution mass spectrometry (MS) spectra were obtained using electrospray ionization (ESI) on an Agilent Series 1100 LC equipped with a photodiode array detector and a 1946 MSD or an Agilent 6545 LC/Q-TOF, respectively. Low-res MS data was analyzed using ChemStation software (Agilent). High-res MS data was analyzed using MassHunter Workstation (Agilent). Molecular formulas were predicted based on HRMS data using ChemCalc (chemcalc.org).<sup>34</sup> Analytical HPLC was performed on an Agilent 1100 HPLC system equipped with a photodiode array detector. HPLC mobile phase consisted of ultra-pure H<sub>2</sub>O (A) and MeCN (B) with 0.05% formic acid in each. A gradient method from 10% to 100% B over 35 minutes at a flow rate of 0.8 mL/min was used. The column (Phenomenx kinetex C18, 5  $\mu$ m, 150 x 6 mm) was re-equilibrated before each injection and the column compartment maintained at 30°C throughout each run. Preparatory HPLC (Phenomenx Luna C18, 5  $\mu$ m, 250 x 21.2 mm) was operated at room temperature using isocratic or gradient elution systems with a flow rate of 20 mL/min. All samples were filtered through a 0.45  $\mu$ m nylon filter or by centrifugation before LCMS and HPLC analysis. NMR spectra were obtained on either a Bruker Avance III 500 MHz or Bruker Avance III 700 MHz spectrometer equipped with a 5 mm TXI probe or <sup>13</sup>C cryoprobe, respectively. Residual solvent was used as an internal standard.

## Microbial cultures

All cultures were grown in a nutrient rich malt media (M2) containing malt extract (10 g/L), yeast extract (4 g/L), and glucose (4 g/L) with the pH adjusted to 6.0 prior to sterilization. For agar plates, 17 g/L agar was added to the growth media prior to sterilization. Bacterial library cultures were prepared by inoculating 250 mL malt broth using a 1 cm<sup>2</sup> piece of five to ten-day old agar followed by cultivation at 28 °C for 14 days on an orbital shaker at 120 rpm. Extracts from 250 mL

cultures exhibiting DNA binding properties were grown in large scale by inoculating a 500 mL broth culture with 50 mL of inoculum grown for 5 days. Cultures were then grown for seven days and used to inoculate up to 14 L of malt-based broth. Large cultures were grown for 14 days at 28 °C on an orbital shaker at 120 rpm.

### **Microbial culture extraction**

All cultures were clean streaked on M2 agar plates prior to extraction to test for strain purity. Small microbial cultures were extracted using an equal volume of ethyl acetate followed by drying over MgSO<sub>4</sub> and concentration under reduced pressure. Large microbial cultures were extracted using absorbing Amberlite XAD-7 resin (Fisher Scientific) by adding it to cultures 24 hours prior to extraction. Resin and mycelia were collected using cheese cloth filtration. Resin and mycelia were soaked in 2 L of a 1:1 methanol/acetone mixture followed by concentration under reduced pressure. Remaining water/extract residue was further extracted three times with ethyl acetate and dried over MgSO<sub>4</sub> followed by concentration under vacuum. Extracts were fractionated over silica using vacuum liquid column chromatography (VLCC) with a gradient of DCM/MeOH. Fractionated extracts were solubilized in DMSO at 10 mg/mL and stored at -20 °C in 96 well plates for screening.

### **DNA oligonucleotides**

DNA oligonucleotides were ordered as complementary single strand segments in 75% GC or AT rich variants (IDT, Coralville, IA). One strand of either the GC or AT DNA variants contained a 5' biotin tag for biosensor immobilization. DNA sequences d(5'-biotin-GATTTCAAGATATTAAGAAG-3') and d(5'-CTTCTTAATATCTTGAAATC-3') were used for AT rich binding analysis while d(5'-biotin-GTGCCTGGACCGCCCGACCT-3') and d(5'-AGGTCGGGCGGTCCAGGCAC-3') were used for GC rich binding analysis. Each

oligonucleotide contained 20 base pairs allowing for the natural formation of two helical twists.<sup>29</sup> The oligomers were designed to avoid intramolecular hairpins, self-dimerization, and cross-dimerization with  $\Delta G$  values of -0.16, 1, -0.13, -0.66 kcal/mol at 25°C, respectively (more negative  $\Delta G$  values represents increased stability). Single stranded DNA oligomers were annealed for 2 min at 94° C followed by cooling to room temperature over 1 hour. Duplex DNA was then stored at -20°C as a 20  $\mu$ M solution in TE buffer (10 mM Tris, 0.5 mM EDTA, 50 mM NaCl, pH 8) until use.

### **Bi-layer Interferometry**

DNA binding events were detected and monitored in real time using a FortéBio Octet Red 96 Bi-layer Interferometer (Molecular Devices). Biotinylated, double-stranded DNA fragments were immobilized on streptavidin (SA) sensor tips for 1600 seconds at 25 nM in 1x Kinetics Buffer. Extracts were screened after resuspension in Kinetics Buffer at 100  $\mu$ g/mL and 5% DMSO. Positive binding hits were identified with binding responses of at least 0.025 nm that reached equilibrium (plateaued binding). The binding affinity ( $K_D$ ), defined as the concentration of analyte required to occupy 50% of the surface ligand sites at equilibrium,<sup>35</sup> was determined for each compound through a dilution series analysis over a concentration range of roughly 0.1  $K_D$  to 100  $K_D$ . Compound testing was done sequentially using baseline, association, and dissociation steps for 30s, 30s, and 60s, respectively. Data was aligned using baseline signal and curves fitted with a 1:1 best-fit model in FortéBio's data analysis software.

### **BLI reference subtraction**

Microbial extracts may contain hundreds of small molecules covering a broad range of polarities, molecular weights, and functional groups.<sup>36</sup> Therefore, screening microbial extracts can create significant atypical binding events to either the sensor itself or to the immobilized DNA

through nonspecific aggregating effects. To reduce signal associated with these atypical binding events as well as potential optical interferences from variations in buffer and signal drift, we utilized reference sensor subtraction.<sup>23,28</sup> A separate set of blank sensors without the DNA load was exposed to the assay conditions and sensors loaded with DNA were placed in buffer wells for signal subtraction.

### Screening assay robustness

We quantified the robustness of the DNA-binding assay using  $Z'$ -factor calculations. A  $Z'$ -factor is used to show whether an assay can reliably distinguish positive and negative samples by comparing the responses of control compounds against the a measurement standard deviation.<sup>37-39</sup> We used doxorubicin (**2**) as a model compound in this analysis. **2** was spiked into an extract without DNA-binding properties at increasing concentrations and the  $Z'$ -factor was calculated according the equation:

$$Z' = 1 - \frac{3\sigma_s + 3\sigma_b}{\mu_s - \mu_b}$$

where  $\sigma_s$  and  $\sigma_b$  represent the standard deviations of both the sample and blank, respectively, and  $\mu_s$  and  $\mu_b$  represent the average of signals from triplicate reads associated with the sample and blank, respectively. For our negative control, we used a non-DNA-binding sample extract at 100  $\mu\text{g/mL}$ . For test solutions, we used **2** at concentrations of 1, 2, 4, 8, 16, 24, 48, 92, and 100  $\mu\text{g/mL}$ , adding a quantity of the non-binding extract to each sample that maintained the total material constant at 100  $\mu\text{g/mL}$  (**Figure 6**). It is customary to take  $Z' > 0.8$  as an indication that the assay reliably distinguishes positive and negative samples,  $Z' > 0.6$  as marginally distinguishing positive and negative samples, and  $Z' < 0.5$  as indicating that the assay is unsuitable for high-throughput screening.<sup>37,38</sup>

### Isolated compounds

Echinomycin (**8**): White solid; UV (MeCN)  $\lambda_{\max}$  (log  $\epsilon$ ) 244, 324 nm;  $^1\text{H}$  NMR (700 MHz,  $\text{CDCl}_3$ )  $\delta$  9.64 (s, 1 H), 9.63 (s, 1 H), 8.84 (d,  $J=6.1$  Hz, 1 H), 8.66 (d,  $J=7.2$  Hz, 1 H), 8.18 (dd,  $J=13, 8.5$  Hz, 2 H), 7.99 (d,  $J=8.2$  Hz, 1 H), 7.94 (d,  $J=8.7$  Hz, 1 H), 7.86 (m,  $J=7.8$  Hz, 2 H), 7.81 (m, 2 H), 6.97 (d,  $J=5.8$  Hz, 1 H), 6.83 (s, 1 H), 6.48 (d,  $J=8.6$  Hz, 1 H), 6.13, (s, 1 H), 5.20 (d,  $J=10.3$  Hz, 1 H), 5.15 (d,  $J=9.9$  Hz, 1 H), 95 (m, 3 H), 82 (m, 2 H), 68 (m, 4 H), 3.43 (d,  $J=15.1$  Hz, 1 H), 3.18 (s, 3 H), 3.10 (s, 3 H), 3.00 (s, 3 H), 2.99 (s, 3H), 2.87 (dd,  $J=16.2, 11.8$  Hz, 1 H), 2.35 (m, 2 H), 2.09 (s, 3 H), 1.41 (d,  $J=6.8$  Hz, 3 H), 1.37 (d,  $J=7.0$  Hz, 3 H), 1.09 (t,  $J=6.2$  Hz, 6 H), 0.92 (d,  $J=6.7$  Hz, 3 H), 0.88 (d,  $J=6.7$  Hz, 3 H); MS (ESI+)  $m/z$  1101.2 ( $\text{M}+\text{H}$ )<sup>+</sup>, 1053.2 ( $\text{M}-\text{SCH}_3$ )<sup>+</sup>; HRMS (ESI+)  $m/z$  1101.4298 ( $[\text{M}+\text{H}]^+$ , calcd. for  $\text{C}_{51}\text{H}_{65}\text{N}_{12}\text{O}_{12}\text{S}_2$ : 1101.4286,  $\Delta\text{ppm}$  1.6).

Actinomycin V (**9**): Orange solid; UV (MeCN)  $\lambda_{\max}$  (log  $\epsilon$ ) 214, 242, 444 nm;  $^1\text{H}$  NMR (500 MHz,  $\text{CDCl}_3$ )  $\delta$  8.15 (d,  $J=5.9$  Hz, 1 H), 7.70 (d,  $J=6.0$  Hz, 1 H), 7.65 (m, 1H), 7.62 (d,  $J=7.8$  Hz, 1 H), 7.36 (d,  $J=7.7$  Hz, 1 H), 7.18 (d,  $J=7.1$  Hz, 1 H), 6.57 (d,  $J=10.5$  Hz, 1 H), 5.96 (d,  $J=9.0$  Hz, 1 H), 5.24 (dd,  $J=6.4, 2.4$  Hz, 1 H), 5.15 (dd,  $J=6.4, 2.4$  Hz, 1 H), 71 (d,  $J=17.8$  Hz, 1 H), 71 (d,  $J=18.8$  Hz, 1 H), 57 (m, 3 H), 49 (m, 1 H), 3.98 (d,  $J=19.3$  Hz, 2 H), 3.87 (m, 3 H), 3.71, (m, 3 H), 3.64 (d,  $J=17.8$  Hz, 3 H), 3.57 (dd,  $J=9.3, 6.3$  Hz, 1 H), 2.93 (s, 3 H), 2.92 (s, 3 H), 2.90 (s, 3 H), 2.89 (s, 3 H), 2.76 (m, 3 H), 2.70 (m, 2 H), 2.65 (m, 2 H), 2.32 (d,  $J=17.3$  Hz, 2 H), 2.17 (m, 6 H), 1.85 (m, 1 H), 1.26 (m, 3 H), 1.13 (m, 9 H), 0.98 (d,  $J=5.8$  Hz, 3 H), 0.95 (d,  $J=5.7$  Hz, 3 H), 0.92 (d,  $J=6.4$  Hz, 3 H), 0.90 (d,  $J=6.4$  Hz, 3 H), 0.75 (d,  $J=6.0$  Hz, 3 H), 0.74 (d,  $J=6.0$  Hz, 3 H); MS (ESI+) 1269.4 ( $\text{M}+\text{H}$ )<sup>+</sup>, 1291.4 ( $\text{M}+\text{Na}$ )<sup>+</sup>; HRMS (ESI+)  $m/z$  1291.5992 ( $[\text{M}+\text{Na}]^+$ , calcd. for  $\text{C}_{62}\text{H}_{84}\text{N}_{12}\text{NaO}_{17}$ : 1291.5975,  $\Delta\text{ppm}$  1.7).

Chartreusin (**10**): Greenish yellow solid; UV (MeCN)  $\lambda_{\text{max}}$  (log  $\epsilon$ ) 236, 266, 334, 402, 424 nm;  $^1\text{H}$  NMR (700 MHz,  $\text{CDCl}_3$ )  $\delta$  11.62 (s, 1 H), 8.20 (d,  $J=8.2$  Hz, 1 H), 7.60 (t,  $J=8.2$  Hz, 1 H), 7.51 (d,  $J=8.4$  Hz, 1 H), 7.44 (d,  $J=7.8$  Hz, 1 H), 7.40 (d,  $J=8.4$  Hz, 1 H), 5.72 (d,  $J=4$  Hz, 1 H), 5.33 (d,  $J=7.4$  Hz, 1 H), 5.11 (s, 2 H), 2.7 (t,  $J=8.2$  Hz, 1 H), 1.9 (q,  $J=6.5$  Hz, 1 H), 3.94 – 3.86 (m, 4 H), 3.78 (dd,  $J=9.2, 3.5$  Hz, 1 H), 3.36 (s, 3 H), 3.35 (s, 3 H), 3.31 (dd,  $J=9.8, 2.8$  Hz, 1 H), 2.81 (s, 3 H), 1.45 (d,  $J=6.5$  Hz, 3 H), 1.40 (d,  $J=6.5$  Hz, 3 H); MS (ESI+)  $m/z$  663.0 ( $\text{M}+\text{Na}$ ) $^+$ .

## Results

### DNA selection and immobilization on BLI sensors

DNA oligonucleotides were designed for binding analysis by BLI following three guidelines. First, the length of the oligonucleotides had to be long enough to contain multiple helical turns. Second, the DNA sequences chosen had to avoid unexpected hairpin loop formation and self/cross dimerization. Third, both GC and AT rich variants of the DNA oligonucleotides were designed to evaluate DNA binding specificity which has been found for several small molecules. Sequences were thus designed as single stranded 20 base oligonucleotides allowing for two helical twists. Subsequent annealing resulted in 75% GC or AT rich double-stranded DNA. The leading strand included a 5' biotin tag for immobilization of the hybridized DNA onto streptavidin coated BLI biosensor tips.

To detect binding events using BLI, the optimal concentration of immobilized DNA ligand needed to be identified.<sup>28</sup> While the loading of too little ligand (DNA bait) can result in insufficient signal-to-noise ratios, the loading of excessively high concentrations of ligand can lead to distortion of binding kinetics at near-saturating concentrations. In general, a slow-linear loading profile of ligand is preferred as it leads to uniform substrate immobilization across the sensor tip while also avoiding distortion of binding curves at saturating analyte concentrations.<sup>28</sup> In **Figure**

**3A**, double-stranded GC rich DNA was immobilized onto streptavidin coated biosensor tips at increasing concentrations of 10, 25, 50, 100, and 200 nanomolar. The highest concentrations of GC rich DNA loaded, 100 and 200 nM, gave steep curves that resulted in the strongest binding signal when tested with doxorubicin (**2**) ( $K_D = 3.3 \times 10^{-7} \text{ M}$ )<sup>40</sup> (**figure 3B**). However, at these concentrations distortion of the binding curves can be seen evident by the signals not reaching a plateaued binding equilibrium during the association phase, which can prevent proper data fitting. Conversely, with a low protein loading concentration of 10 nM GC DNA, no binding distortion was observed but the overall response during association with **2** was reduced. Thus, DNA loading concentrations of 25 nM were chosen for the remainder of experiments as it resulted in binding profiles that reach equilibrium during association and avoided binding distortion while still providing good signal-to-noise resolution.

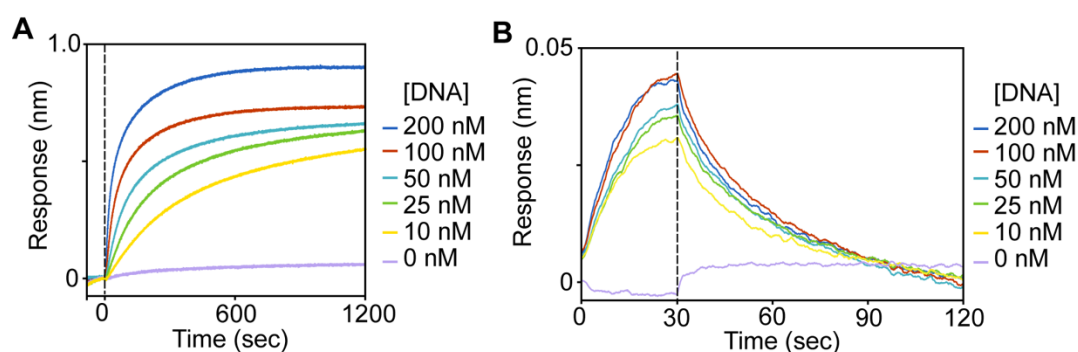


**Figure 3:** DNA immobilization concentration tests using GC rich DNA bound to streptavidin biosensors. **(A)** Duplex GC DNA with a 5' biotin tag was immobilized onto streptavidin sensors at 0, 10, 25, 50, 100, and 200 nM. Buffer baseline and DNA loading steps are shown from left to right, respectively. **(B)** Association of doxorubicin (1  $\mu\text{M}$ ) to DNA loaded sensors. Sensors with high levels of loaded DNA show distortion of binding curves and do not reach a state of equilibrium (plateaued binding). Sensors with less DNA (25, 50 nM) show optimal association curves by reaching a state of equilibrium with sufficient signal-to-noise levels. Association and dissociation steps shown from left to right, respectively.

## Binding affinity of known DNA acting agents

To verify the utility of BLI for measuring the binding affinity of small molecules to DNA, we sought to characterize the binding affinities ( $K_D$ ) of known DNA intercalating, groove binding, and covalent binding agents with subsequent comparisons of their  $K_D$  values to published values derived from different analytical methods (e.g. ITC and SPR). The DNA intercalating agents tested included actinomycin D (**1**), doxorubicin (**2**), ethidium bromide (**3**), and propidium iodide (**4**). The DNA minor groove binding agents tested included the dye Hoechst 33342 (**5**) and netropsin (**6**) (**Figure 1**). Additionally, cisplatin (**7**), a DNA covalent binding agent, was tested for DNA binding. DNA affinities were calculated using a 1:1 global binding analysis of BLI sensorgrams for each compound tested over a range of concentrations ranging from around  $0.1 K_D$  to  $100 K_D$  (**Figure 4**). These values were then compared to previously reported binding affinities (**Table 1**). Acetylcysteine and ascorbic acid were used as negative binding controls and predictably showed no binding to either GC or AT rich DNA at any concentration tested (**Figure S1**).

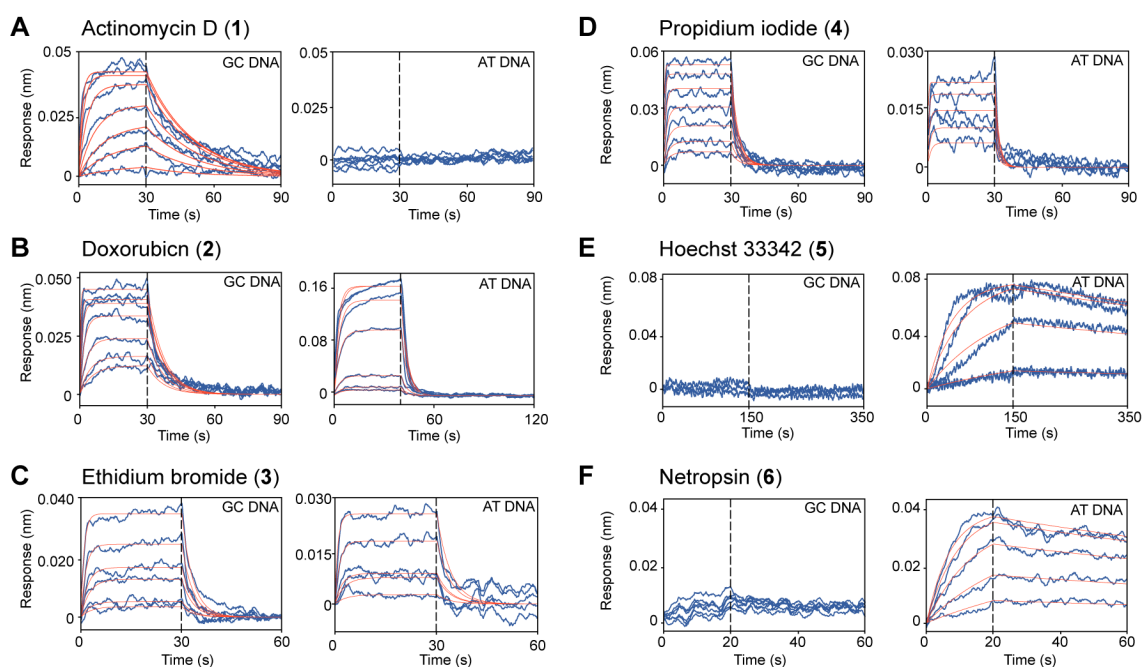


**Figure 4:** Sensorgrams of known DNA intercalating and groove binding agents against GC and AT rich DNA. (A) Actinomycin D was tested at 0.03, 0.10, 0.20, 0.40, 1.00, 2.00, and 3.00  $\mu\text{M}$ . (B) Doxorubicin was tested at 0.08, 0.16, 0.31, 0.63, 1.25, 2.50, and 5.00  $\mu\text{M}$ . (C) Ethidium bromide was tested at 0.16, 0.31, 0.63, 1.25, 2.50, and 5.00  $\mu\text{M}$ . (D) Propidium iodide was tested at 0.16, 0.31, 0.63, 1.25, 2.50, 5.00, and 10.00  $\mu\text{M}$ . (E) Hoechst 33342 was tested at 0.10, 0.25, 0.50, and 0.75  $\mu\text{M}$ . (F) Netropsin was tested at 0.10, 0.25, 0.50, 0.75, and 1.00  $\mu\text{M}$ .

**Table 1:** Binding affinities of known DNA binding compounds

	GC DNA (M)	AT DNA (M)	Literature $K_D$ (M)*
actinomycin D	$2.3 \times 10^{-7}$	ND**	$2.0 \times 10^{-7}$
doxorubicin	$2.5 \times 10^{-7}$	$2.0 \times 10^{-5}$	$3.3 \times 10^{-7}$
ethidium bromide	$3.7 \times 10^{-6}$	$1.4 \times 10^{-6}$	$1.5 \times 10^{-5}$
propidium iodide	$1.2 \times 10^{-6}$	$5.6 \times 10^{-6}$	$5.3 \times 10^{-7}$
Hoechst 33342	ND**	$3.7 \times 10^{-8}$	$5.6 \times 10^{-8}$
netropsin	ND**	$3.1 \times 10^{-8}$	$4.2 \times 10^{-7}$

\*Literature sources: actinomycin D<sup>41</sup>, doxorubicin<sup>40</sup>, ethidium bromide<sup>42</sup>, propidium iodide,<sup>43</sup> Hoechst 33342<sup>15</sup>, netropsin<sup>15</sup>

\*\*Binding not detected at any concentration

DNA intercalating agents have been shown to have a moderate to strong preference binding GC rich DNA by fitting between alternating pyrimidine-purine sites.<sup>44</sup> Indeed, the two natural product sourced DNA intercalating agents tested in this study, actinomycin D (**1**) and doxorubicin (**2**), both showed strong preference for GC rich DNA. Particularly, **1** showed complete selectivity to our model GC rich oligonucleotide with a binding affinity of  $2.3 \times 10^{-7}$  M while showing no binding to AT rich DNA at any concentration tested. Previous reports found **1** to bind DNA with an affinity around  $2.0 \times 10^{-7}$  M, depending on the length and percent GC content of the DNA tested.<sup>41</sup> Other reports found the binding affinity of **1** as weak as  $3.3 \times 10^{-6}$  M when tested against salmon sperm DNA using reflectometric interference spectroscopy.<sup>39</sup> The more than 10 fold reduction in affinity compared to results reported herein are likely due the DNA source used in their experiments, salmon sperm, which has a GC content of less than 50%.<sup>40,45</sup>

Doxorubicin (**2**) showed strong preference to GC rich DNA with a binding affinity of  $2.5 \times 10^{-7}$  M. Binding to AT rich DNA, however, only resulted in an affinity of  $2.0 \times 10^{-5}$  M. Previously,

when tested by Phieler et al. for binding to salmon sperm DNA, **2** gave a binding affinity to GC DNA slightly lower than our results at  $3.3 \times 10^{-7}$  M.<sup>40</sup> This difference is, once again, likely due to the low GC content in the salmon sperm DNA used.<sup>40</sup> Against AT rich DNA, **2** gave a low  $K_D$  in line with previous reports,<sup>46</sup> but also showed unsaturated binding behavior at higher concentrations, most likely due to atypical binding effects associated with aggregation or other secondary binding events.<sup>25</sup>

The synthetic DNA intercalators ethidium bromide (**3**) and propidium iodide (**4**) bound equally well to GC and AT rich DNA. Compound **3** exhibited a slightly tighter affinity to AT over GC rich DNA with  $1.4 \times 10^{-6}$  M and  $3.7 \times 10^{-6}$  M, respectively. However, these affinities to both GC and AT rich DNA were significantly stronger than the previously reported  $K_D$  value  $1.5 \times 10^{-5}$  M obtained when using calf thymus DNA and ITC.<sup>42</sup> This 10 fold discrepancy is likely due to the previously reported values being determined using ITC, which is known to be sensitive to different substrates, changes in buffer, temperature, and pH conditions.<sup>26</sup> Compound **4** showed similar binding to both GC and AT rich DNA with only a slight preference to GC DNA with affinities of  $1.2 \times 10^{-6}$  M and  $5.6 \times 10^{-6}$  M, respectively. Using UV melting curves, Chou et. al. calculated a binding affinity of  $5.3 \times 10^{-7}$  M against salmon teste DNA. However, in the same study **4** gave a  $K_D$  of  $2.8 \times 10^{-6}$  M against AT rich DNA polymers at high salt concentrations which closely matches results obtained using BLI.<sup>43</sup>

Two minor groove binding agents were tested for DNA binding including Hoechst 33342 (**5**) and netropsin (**6**). In general, minor groove binding agents are known to show binding selectivity to AT rich over GC rich DNA as adenine-thymine base pairs offer increased electrostatic interactions in their minor groove that allow for tighter binding to positively charged molecules (e.g. Hoechst 33342).<sup>47-49</sup> As expected, **5** and **6** both showed strong binding affinities to AT DNA

with  $K_D$ 's of  $3.7 \times 10^{-8}$  M and  $3.1 \times 10^{-8}$  M, respectively. No binding of either compound to GC rich DNA was observed at any concentration tested. Hoechst's (**5**) binding affinity closely matched a previously determined affinity by Bailly et al. using SPR with a designed 20-mer DNA oligonucleotide that resulted in a calculated  $K_D$  of  $5.6 \times 10^{-8}$  M.<sup>47</sup> Conversely, netropsin's (**6**)  $K_D$  was previously determined to be  $4.2 \times 10^{-7}$  M using ITC, an order of magnitude weaker than the  $K_D$  of  $3.1 \times 10^{-8}$  M we determined using BLI.<sup>47,48,50</sup> In addition to the different method used to determine the affinity of **6** (BLI vs ITC), this study designed double-stranded DNA with a 75% AT composition, making it especially well-suited for minor groove binding agents likely resulting in the observed tighter affinity value.

Lastly, we tested cisplatin (**7**), a therapeutically relevant DNA binding agent, which covalently binds to DNA. Monitoring covalent binding events offer unique challenges including their relatively slow binding kinetics as well as permanent changes made to the DNA upon binding.<sup>51</sup> Nonetheless, using an extended association time of 1600 seconds, compared to 30 seconds for other small molecules, we were able to identify binding events between DNA and **7** against both GC and AT rich DNA (**Figure 5**). BLI sensorgrams showed substantially reduced dissociation consistent with covalent binding, which also precluded calculation of a binding affinity. However, the unique BLI sensorgrams easily allowed for the identification of DNA covalent binding events, which may allow the identification of covalent binding agents from complex mixtures in the future.

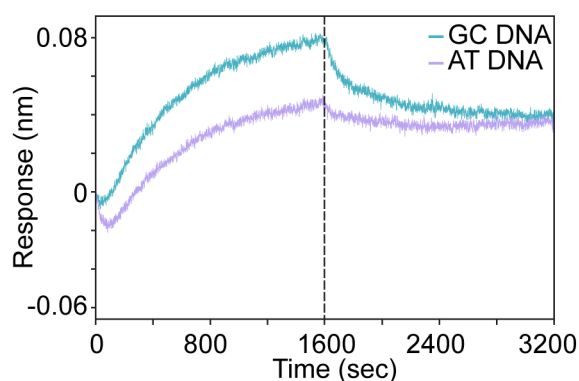


**Figure 5:** Binding of cisplatin (**7**, 125  $\mu$ M) to both GC and AT rich DNA. Sensorgram includes both association (left) and dissociation (right) of **7** to DNA.

Using designed duplex oligonucleotides with 75% GC or AT content, we were able to robustly characterize the binding affinity of six different DNA intercalating and minor groove binding agents. Additionally, we were able to detect covalent binding of cisplatin to both GC and AT rich DNA. BLI's dip-and-read approach only requires small amounts of DNA bait while the use of the commercially available GC/AT rich DNA oligonucleotides enables comparative analyses across laboratories. BLI performed exceptionally well for small molecule-DNA binding identification with each pure compound tested resulting in reproducible binding kinetics while covering a large range of binding affinities, ranging here from  $2.0 \times 10^{-5}$  –  $3.1 \times 10^{-8}$  M.

### **Screening of microbial extracts for DNA binding**

Identifying individual active-compounds from microbial extracts is intrinsically challenging due to the highly complex nature of natural product extracts that typically feature a wide range of compounds with differing molecular weights, polarities, concentrations, and pH.<sup>36,52,53</sup> Early ligand-based screening using biosensor technology for DNA binding offers several advantages. First, it is faster and cheaper than phenotypic assays in its prediction of cell toxicity compared to mammalian cell-based assays. DNA binding can serve as a tool to detect new chemotherapeutics but also function as a counter screen for unwanted toxicity in campaigns for new drug leads in other areas, for example infectious diseases. Second, Biolayer Interferometry is especially well suited to screening microbial extract libraries with its 96 or higher well plate format utilizing dip-and-read biosensors without microfluidics. Additionally, less analyte is required to coat biosensor tips and the optical monitoring properties of BLI make it more resistant to changes in the refractive index and pH from sample to sample.<sup>54</sup> Nevertheless, to develop BLI into a successful screening

tool for microbial extracts, parameters including limit of detection, avoidance of unspecific binding, and best practice for data analysis needed to be established.

We first sought to identify the limit of detection of DNA binding metabolites within microbial extracts. Model compound doxorubicin (**2**) was spiked into a microbial extract (*Streptomyces* strain O1/4, inactive in DNA-binding assays) to create 100  $\mu\text{g/mL}$  samples with increasing concentrations by weight (w/w) of **2** (**Figure 6**). The spiked extracts were then analyzed by BLI in triplicate to identifying DNA binding against GC rich DNA. To assess the detection limit cutoff,  $Z'$ -factors were calculated for each sample based on the maximum signal response (**Table 2**). Testing against GC rich DNA showed that **2** could be identified with a sufficient  $Z'$ -factor ( $>0.6$ ) in all but the lowest sample concentration (1% w/w). In fact, when just 4% of the extract mass was attributed to compound **2**, the  $Z'$ -factor was 0.85, making **2** easily identifiable at that screening concentration. However, when tested against AT rich DNA, **2** does not have a strong binding affinity ( $2.0 \times 10^{-5}$  M). This is reflected by the poor  $Z'$ -factor of only 0.35 at concentrations as high as 8% (w/w). Based on this data, we determined that compounds with a high binding affinity to DNA ( $<1.0 \times 10^{-6}$  M) can be detected in exceedingly low concentrations of just 2% w/w of the total extract. Lower affinity compounds however ( $>1.0 \times 10^{-6}$  M), may only be detectable if they are the major component of the extract ( $>16\%$  w/w).

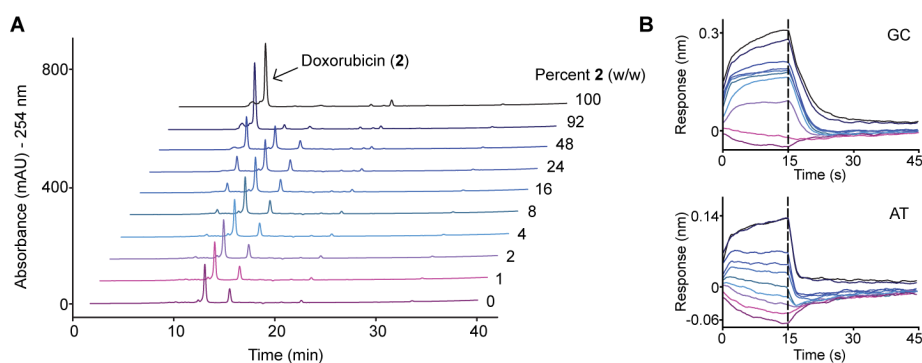


**Figure 6:** Extract from *Streptomyces* O1/4, which does not exhibit DNA binding properties to GC or AT rich DNA, was spiked with doxorubicin (**2**) in increasing concentration to test for

BLI's limit of detection. (A) LCMS chromatogram of O1/4 spiked with increasing concentrations of **2** by weight (w/w) (**2** elutes at 12 min). (B) Binding sensorgrams of each O1/4 - doxorubicin spiked extract against GC and AT rich DNA with line colors correlating to w/w concentrations of **2** as listed.

**Table 2:** Limit of detection by Z'-factors

Percent doxorubicin in extract (w/w)	Z'-factors*	
	GC-DNA	AT-DNA
0	-	-
1	-	-
2	0.70	-
4	0.85	-
8	0.84	0.35
16	0.87	0.65
24	0.89	0.77
48	0.83	0.76
92	0.90	0.88
100	0.86	0.86

\*Z'-factors less than 0.5 are statistically poor, greater than 0.6 are marginal, and greater than 0.8 excellent.

### Identification of small molecule binders from microbial extracts

We utilized our validated BLI-DNA binding screening system to analyze an in-house library of bacterial extracts and fractions. In total, over 100 bacterial extracts were examined for binding against both GC and AT rich DNA. For each extract tested, double reference subtraction was used to subtract the effects from unspecific binding. Extract O1/8 derived from a *Streptomyces* sp., showed strong-preferential binding to GC rich DNA in initial screening and was thus further tested for binding activity. After initial silica separations, each fraction was tested for binding at 100 µg/mL resulting in fractions 2 and 3 identified with positive binding responses of 0.06 to 0.08 nm (Figure 7). Chemical analysis of the active binding fraction 3 from extract O1/8 by LCMS indicated only one primary compound present. Chromatographic isolation techniques followed by compound identification via HRMS and NMR analysis identified this compound as the peptide

antibiotic echinomycin (**8**, [Figures S4-S7]). **8** is a well-known DNA bis-intercalator with a preference to bind GC rich DNA.<sup>55,56</sup> In our hands, **8** bound to GC and AT DNA with affinities of  $7.1 \times 10^{-7}$  M and  $>1.0 \times 10^{-4}$  M, respectively. This is a much stronger binding affinity to GC rich DNA than a previously reported affinity of  $1.8 \times 10^{-6}$  M as reported from UV melting curve studies using herring sperm DNA (Table 3).<sup>55</sup> Additionally, LCMS based analysis of extract O1/8 fraction 2 showed multiple metabolites with UV profiles identical to **8** but featuring differing molecular weights (data not shown); these compounds are potentially derivatives of echinomycin and most likely responsible for the binding properties associated with fraction 2.

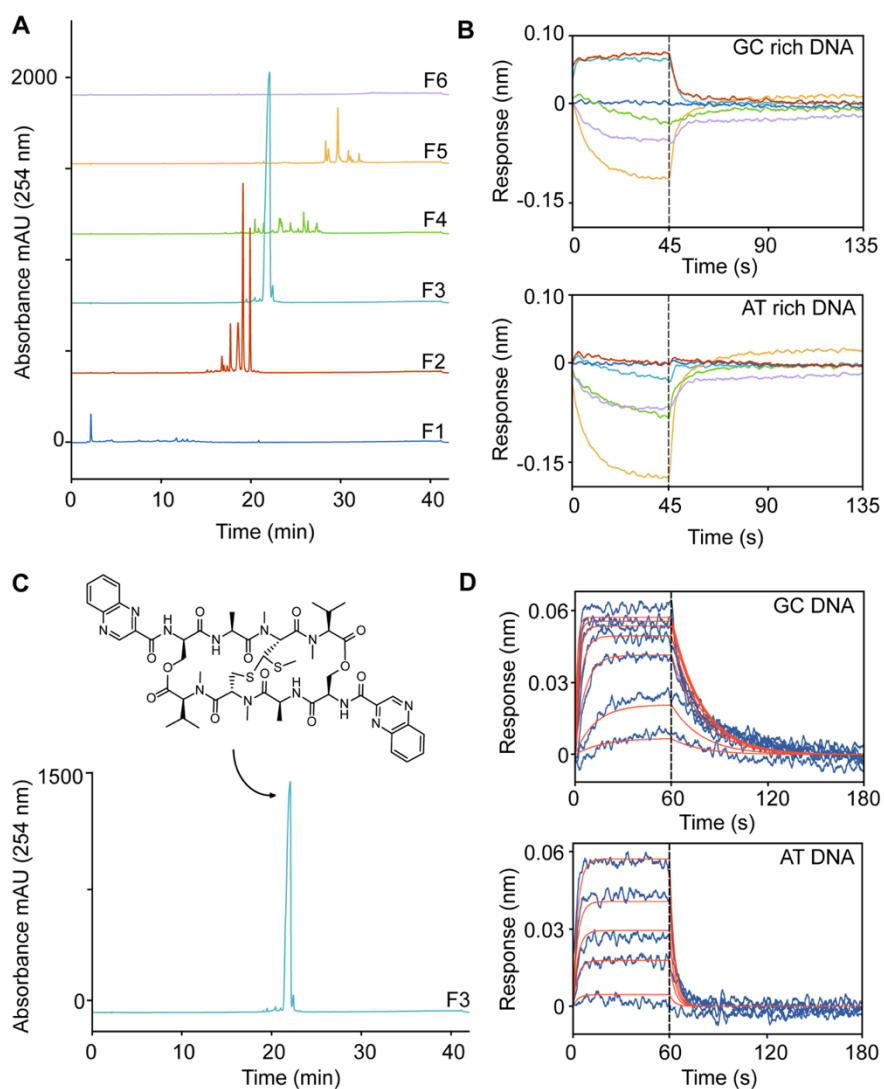


**Figure 7:** Identification and isolation of the DNA intercalator echinomycin (**8**) from microbial extract screening. (A) HPLC chromatogram of fractions from *Streptomyces* strain O1/8 at 254 nm wavelength. (B) Binding analysis of fractions. Fractions 2 (red) and 3 (blue) show significant binding to GC rich DNA. (C) Fraction 3 (blue) shows one major component identified as echinomycin (**8**). (D) Purified echinomycin (**8**) binding to GC rich and AT rich DNA at 0.09, 0.37, 1.50, 3.00, 5.00, 7.00, and 10.00  $\mu\text{M}$ .

Another bacterial extract, RM1-1, was identified from library screening with binding curves to both GC and AT rich DNA. Six fractions of RM1-1 were produced and screened for binding to both GC and AT DNA (**Figure 8**). Fractions 5 and 6 exhibited strong binding to GC and AT DNA with responses of 0.15 nm and 0.3 nm, respectively. Fraction 6, as analyzed by LCMS, exhibited three components of which the major was identified as actinomycin V (**9**) by HRMS and NMR examination (**Figure S8**). After purification, affinity testing showed that **9** tightly bound GC rich DNA with an affinity of  $2.0 \times 10^{-7}$  M, similar to the affinity of its structural analog actinomycin D (**1**) ( $2.3 \times 10^{-7}$  M, [**Table 1**]).

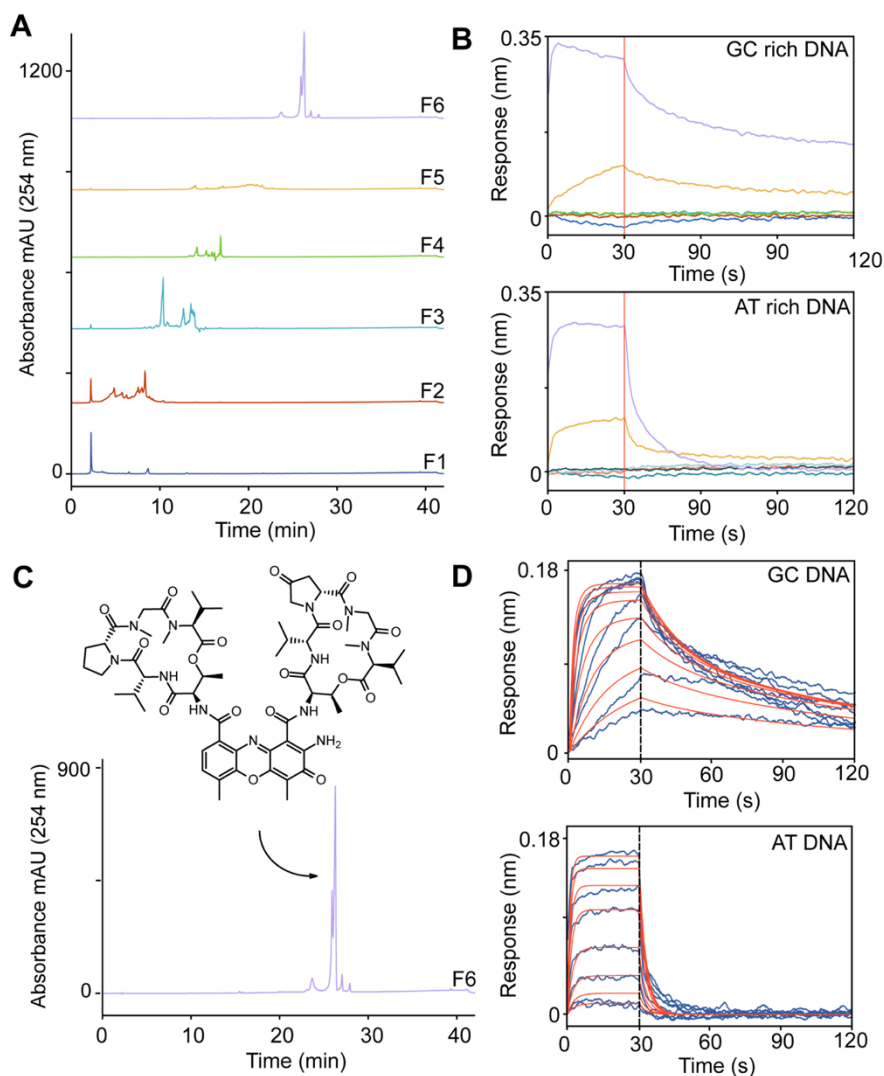


**Figure 8:** Binding-guided isolation of actinomycin V (**9**). (A) HPLC chromatograms of fractions from RM1-1 extract at 254 nm wavelength. (B) Binding analysis of fractions. Fractions 5 (orange) and 6 (purple) show binding to GC and AT rich DNA. (C) Fraction 6 (purple) shows one major component identified as actinomycin V (**9**). (D) Purified actinomycin V (**9**) binding to GC and AT rich DNA at 0.25, 0.50, 1.00, 2.00, 4.00, 6.00, 8.00, and 10.00  $\mu\text{M}$ .

Preferential binding to GC rich DNA was also identified in the extract of bacterium K14/2 with a small binding response of 0.04 nm. Fractionation and testing by BLI showed binding activity mostly in fraction 5 (**Figure 9**). LCMS analysis revealed one major component present with a characteristic UV absorption pattern and molecular mass identical to the natural product chartreusin (**10**). HRMS and NMR were used to confirm the structural assignment. In previous

reports using ITC, compound **10** showed moderate affinity to salmon sperm DNA with a binding affinity of  $2.8 \times 10^{-6}$  M.<sup>57</sup> Using BLI, **10** showed no binding to AT rich DNA at any concentration tested up to 120  $\mu$ M and only a weak binding affinity to GC DNA ( $2.7 \times 10^{-5}$  M).

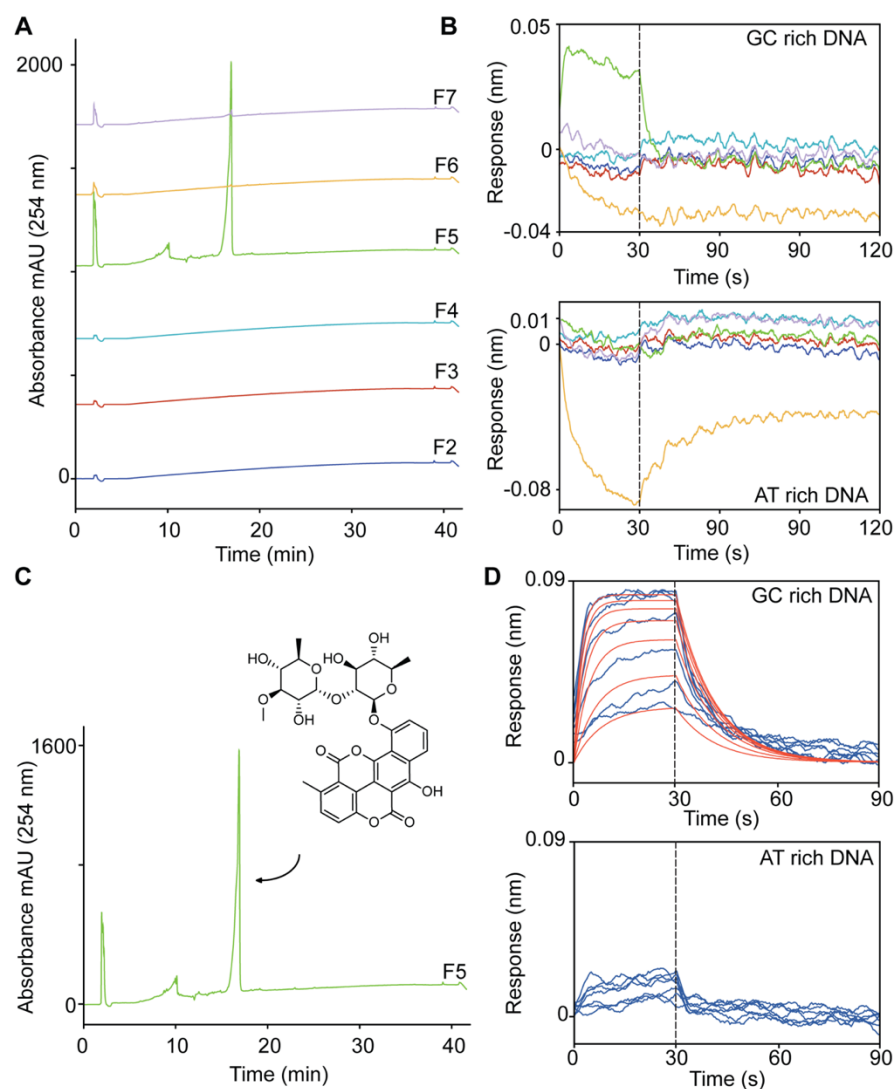


**Figure 9:** Binding-guided isolation of chartreusin (**10**). (A) HPLC chromatogram of fractions from extract K14/2 at 254 nm wavelength. (B) Binding analysis of fractions. Fraction 5 (green) showed binding to GC rich DNA only. (C) Fraction 5 (green) shows one major component identified as chartreusin (**10**). (D) Purified chartreusin (**10**) binding to GC and AT rich DNA at 10, 20, 40, 60, 80, 100, and 120  $\mu$ M.

The compound lumichrome (**11**) was also detected by its retention time, molecular weight, and UV absorption spectrum in the bacterial extract from strain K9/11 during library screening, but we were unable to isolate it due to insufficient material (**Figures S2-S3**). **11** can be derived from the vitamin riboflavin produced in plants and bacteria, often found in microbial media components. **11** has been shown previously to exhibit DNA intercalating properties using LCMS and UV spectroscopy.<sup>58</sup>

**Table 3:** Binding affinities of isolated DNA binding compounds with their related binding affinities from literature

	GC DNA (M)	AT DNA (M)	Literature $K_D$ (M) <sup>*</sup>
Echinomycin	$7.1 \times 10^{-7}$	$1.0 \times 10^{-4}$	$1.8 \times 10^{-6}$
Actinomycin V	$2.0 \times 10^{-7}$	$5.3 \times 10^{-6}$	---
Chartreusin	$2.7 \times 10^{-5}$	ND <sup>**</sup>	$2.8 \times 10^{-6}$

Compounds were greater than 95% pure by LCMS analysis.

<sup>\*</sup>Literature sources: echinomycin<sup>55</sup>, chartreusin<sup>57</sup>

<sup>\*\*</sup>Binding not detected

## Discussion

In conclusion, we present a BLI based assay to detect and quantitate DNA/small molecule binding events. First, the assay was optimized and validated through multiple steps including: 1) optimizing the loading concentrations of DNA, 2) analyzing the effects of non-specific binding through reference subtraction, 3) assessing the robustness of DNA binding identification using Z'-factors, and 4) verifying the capabilities of BLI in measuring binding affinities of commercially available small molecules to DNA. Through this, we found that BLI offers a simple to use, low-cost, and highly effective method in identifying DNA binding agents with medium throughput. We employed our BLI protocol to screen an in-house library of microbial extracts and fractions. In total, over 100 bacterial extracts were screened, and four DNA binding compounds were

identified including the known DNA binding metabolites echinomycin (**8**), actinomycin V (**9**), chartreusin (**10**), and lumichrome (**11**). The BLI assay itself was found to not only be robust when testing extracts of various complexity, but the sensors could be re-used if no binding event or full dissociation was observed, and it can be easily implemented in future screening campaigns to test large libraries of natural or synthetic compounds. While BLI methodology is complementary to other bio-physical techniques available for the detection of DNA-binding, it is uniquely well-suited for dip-and-read screening of complex microbial extracts. In particular, metabolite isolation and identification was highly accelerated using BLI and our designed DNA oligomers, featuring 75% AT and GC content. Nonetheless, like most techniques, screening of microbial extracts is not without obstacles. Low affinity ( $>1.0 \times 10^{-5}$  M) DNA binding agents may be missed if only present in relatively low concentration (less than 8% w/w of an extract). As a solution, we implemented an extract first screen, followed up with screening fractions of the extracts derived from polarity based chromatography to allow for more resolved testing.<sup>59</sup> Further screening of microbial extract libraries using BLI has potential to accelerate the discovery of novel DNA-binding natural products, which could be developed into new therapeutic compounds and/or molecular probes.

### **Acknowledgements**

Thanks to Khaled Attia Mahmoud and Jon Thorson (Center for Pharmaceutical Research and Innovation, Lexington KY) for their kind donation of the bacterial strain RM1-1. Thanks to James A. Strother (UF) for fruitful discussions. We acknowledge the support of the Oregon State University's NMR Facility funded in part by the National Institutes of Health, HEI grant 1S10OD018518, and by the M. J. Murdock Charitable Trust grant no. 2014162. This work was

supported by OSU start-up funds and by the National Science Foundation under grant CHE 1808717.

## References

- (1) Zhu, W.; Wang, Y.; Li, K.; Gao, J.; Huang, C.-H.; Chen, C.-C.; Ko, T.-P.; Zhang, Y.; Guo, R.-T.; Oldfield, E. Antibacterial drug leads: DNA and enzyme multitargeting. *J. Med. Chem.* **2015**, *58*, 1215-1227.
- (2) Bottini, A.; De, S. K.; Wu, B.; Tang, C.; Varani, G.; Pellecchia, M. Targeting influenza a virus RNA promoter. *Chem. Biol. Drug. Des.* **2015**, *86*, 663-673.
- (3) Wang, M.; Yu, Y.; Liang, C.; Lu, A.; Zhang, G. Recent advances in developing small molecules targeting nucleic acid. *Int. J. Mol. Sci.* **2016**, *17*, 779 - 803.
- (4) Cheung-Ong, K.; Giaever, G.; Nislow, C. DNA-damaging agents in cancer chemotherapy: serendipity and chemical biology. *Chem. Biol.* **2013**, *20*, 648-659.
- (5) Müller, S. DNA damage-inducing compounds: Unraveling their pleiotropic effects using high throughput sequencing. *Curr. Med. Chem.* **2017**, *24*, 1558-1585.
- (6) Brockman, H.; Baurer, K. *Naturwissenschaften* **1950**, *37*, 492.
- (7) WilliamáLown, J. Discovery and development of anthracycline antitumour antibiotics. *Chem. Soc. Rev.* **1993**, *22*, 165-176.
- (8) Rescifina, A.; Zagni, C.; Varrica, M. G.; Pistarà, V.; Corsaro, A. Recent advances in small organic molecules as DNA intercalating agents: Synthesis, activity, and modeling. *Eur. J. Med. Chem.* **2014**, *74*, 95-115.
- (9) Lipshultz, S. E.; Herman, E. H. Anthracycline cardiotoxicity: the importance of horizontally integrating pre-clinical and clinical research. *Cardiovasc. Res.* **2018**, *114*, 205-209.
- (10) McGowan, J. V.; Chung, R.; Maulik, A.; Piotrowska, I.; Walker, J. M.; Yellon, D. M. Anthracycline chemotherapy and cardiotoxicity. *Cardiovasc. Drugs Ther.* **2017**, *31*, 63-75.
- (11) Cancer Statistics; Understanding Cancer; National Cancer Institute: cancer.gov, 2018.
- (12) Blum, J. L.; Flynn, P. J.; Yothers, G.; Asmar, L.; Geyer Jr, C. E.; Jacobs, S. A.; Robert, N. J.; Hopkins, J. O.; O'Shaughnessy, J. A.; Dang, C. T. Anthracyclines in Early Breast Cancer: The ABC Trials—USOR 06-090, NSABP B-46-I/USOR 07132, and NSABP B-49 (NRG Oncology). *J. Clin. Oncol.* **2017**, *35*, 2647 - 2655.
- (13) Bozko, M.; Bozko, A.; Scholta, T.; P Malek, N.; Bozko, P. DNA Damage as a Strategy for Anticancer Chemotherapy. *Curr. Med. Chem.* **2017**, *24*, 1487-1487.
- (14) Chaires, J. B. A thermodynamic signature for drug–DNA binding mode. *Arch. Biochem. Biophys.* **2006**, *453*, 26-31.
- (15) Rosu, F.; Gabelica, V.; Houssier, C.; De Pauw, E. Determination of affinity, stoichiometry and sequence selectivity of minor groove binder complexes with double-stranded oligodeoxynucleotides by electrospray ionization mass spectrometry. *Nucleic Acids Res.* **2002**, *30*, e82-e82.
- (16) Cummins, L. L.; Chen, S.; Blyn, L. B.; Sannes-Lowery, K. A.; Drader, J. J.; Griffey, R. H.; Hofstadler, S. A. Multitarget affinity/specificity screening of natural products: finding and characterizing high-affinity ligands from complex mixtures by using high-performance mass spectrometry. *J. Nat. Prod.* **2003**, *66*, 1186-1190.

- (17) Mazzitelli, C. L.; Chu, Y.; Reczek, J. J.; Iverson, B. L.; Brodbelt, J. S. Screening of threading bis-intercalators binding to duplex DNA by electrospray ionization tandem mass spectrometry. *J. Am. Soc. Mass Spectr.* **2007**, *18*, 311-321.
- (18) Geierstanger, B. H.; Jacobsen, J. P.; Mrksich, M.; Dervan, P. B.; Wemmer, D. E. Structural and dynamic characterization of the heterodimeric and homodimeric complexes of distamycin and 1-methylimidazole-2-carboxamide-netropsin bound to the minor groove of DNA. *Biochemistry* **1994**, *33*, 3055-3062.
- (19) Ren, J.; Jenkins, T. C.; Chaires, J. B. Energetics of DNA intercalation reactions. *Biochemistry* **2000**, *39*, 8439-8447.
- (20) Sirajuddin, M.; Ali, S.; Badshah, A. Drug–DNA interactions and their study by UV–Visible, fluorescence spectroscopies and cyclic voltametry. *J. Photochem. Photobiol., B* **2013**, *124*, 1-19.
- (21) Pasternack, R. F.; Bustamante, C.; Collings, P. J.; Giannetto, A.; Gibbs, E. J. Porphyrin assemblies on DNA as studied by a resonance light-scattering technique. *J. Am. Chem. Soc.* **1993**, *115*, 5393-5399.
- (22) Boger, D. L.; Fink, B. E.; Brunette, S. R.; Tse, W. C.; Hedrick, M. P. A simple, high-resolution method for establishing DNA binding affinity and sequence selectivity. *J. Am. Chem. Soc.* **2001**, *123*, 5878-5891.
- (23) Nguyen, B.; Tanious, F. A.; Wilson, W. D. Biosensor-surface plasmon resonance: quantitative analysis of small molecule–nucleic acid interactions. *Methods* **2007**, *42*, 150-161.
- (24) Chaires, J. B. Drug–DNA interactions. *Curr. Opin. Struct. Bio.* **1998**, *8*, 314-320.
- (25) Sultana, A.; Lee, J. E. Measuring Protein–Protein and Protein–Nucleic Acid Interactions by Biolayer Interferometry. *Curr. Protoc. Protein Sci.* **2015**, *79*, 1-26.
- (26) Palchaudhuri, R.; Hergenrother, P. J. DNA as a target for anticancer compounds: methods to determine the mode of binding and the mechanism of action. *Curr. Opin. Biotechnol.* **2007**, *18*, 497-503.
- (27) Wartchow, C. A.; Podlaski, F.; Li, S.; Rowan, K.; Zhang, X.; Mark, D.; Huang, K.-S. Biosensor-based small molecule fragment screening with biolayer interferometry. *J. Comput. Aided Mater. Des.* **2011**, *25*, 669.
- (28) Shah, N. B.; Duncan, T. M. Bio-layer interferometry for measuring kinetics of protein–protein interactions and allosteric ligand effects. *J. Vis. Exp.* **2014**.
- (29) Kachko, A.; Loesgen, S.; Shahzad-UI-Hussan, S.; Tan, W.; Zubkova, I.; Takeda, K.; Wells, F.; Rubin, S.; Bewley, C. A.; Major, M. E. Inhibition of hepatitis C virus by the cyanobacterial protein *Microcystis viridis* lectin: mechanistic differences between the high-mannose specific lectins MVL, CV-N, and GNA. *Mol. Pharm.* **2013**, *10*, 4590-4602.
- (30) Sharma, P.; Tomar, A. K.; Kundu, B. Interplay between CedA, rpoB and double stranded DNA: A step towards understanding CedA mediated cell division in *E. coli*. *Int. J. Biol. Macromol.* **2018**, *107*, 2026-2033.
- (31) Müller-Esparza, H.; Osorio-Valeriano, M.; Steube, N.; Thanbichler, M.; Randau, L. Bio-Layer Interferometry Analysis of the Target Binding Activity of CRISPR-Cas Effector Complexes. *Front. Mol. Biosci.* **2020**, *7*, 98.
- (32) Normand, A.; Rivière, E.; Renodon-Cornière, A. Identification and characterization of human Rad51 inhibitors by screening of an existing drug library. *Biochem. Pharmacol.* **2014**, *91*, 293-300.

- (33) McGrath, T. F.; Campbell, K.; Fodey, T. L.; O’Kennedy, R.; Elliott, C. T. An evaluation of the capability of a bilayer interferometry biosensor to detect low-molecular-weight food contaminants. *Anal. Bioanal. Chem.* **2013**, *405*, 2535-2544.
- (34) Patiny, L.; Borel, A. ChemCalc: a building block for tomorrow’s chemical infrastructure. *J. Chem. Inf. Model* **2013**, *53*, 1223-1228.
- (35) Petersen, R. L. Strategies using bio-layer interferometry biosensor technology for vaccine research and development. *Biosensors* **2017**, *7*, 49.
- (36) David, B.; Wolfender, J.-L.; Dias, D. A. The pharmaceutical industry and natural products: historical status and new trends. *Phytochem. Rev.* **2015**, *14*, 299-315.
- (37) Birmingham, A.; Selfors, L. M.; Forster, T.; Wrobel, D.; Kennedy, C. J.; Shanks, E.; Santoyo-Lopez, J.; Dunican, D. J.; Long, A.; Kelleher, D. Statistical methods for analysis of high-throughput RNA interference screens. *Nat. Methods* **2009**, *6*, 569-575.
- (38) Zhang, J.-H.; Chung, T. D.; Oldenburg, K. R. A simple statistical parameter for use in evaluation and validation of high throughput screening assays. *J. Biomol. Screen.* **1999**, *4*, 67-73.
- (39) Perspicace, S.; Banner, D.; Benz, J.; Müller, F.; Schlatter, D.; Huber, W. Fragment-based screening using surface plasmon resonance technology. *J. Biomol. Screen.* **2009**, *14*, 337-349.
- (40) Piehler, J.; Brecht, A.; Gauglitz, G.; Zerlin, M.; Maul, C.; Thiericke, R.; Grabley, S. Label-free monitoring of DNA–ligand interactions. *Anal. Biochem.* **1997**, *249*, 94-102.
- (41) Hollstein, U. Actinomycin. Chemistry and mechanism of action. *Chem. Rev.* **1974**, *74*, 625-652.
- (42) Nafisi, S.; Saboury, A. A.; Keramat, N.; Neault, J.-F.; Tajmir-Riahi, H.-A. Stability and structural features of DNA intercalation with ethidium bromide, acridine orange and methylene blue. *J. Mol. Struct.* **2007**, *827*, 35-43.
- (43) Chou, W. Y.; Marky, L. A.; Zaunczkowski, D.; Breslauer, K. J. The thermodynamics of drug-DNA interactions: ethidium bromide and propidium iodide. *J. Biomol. Struct. Dyn.* **1987**, *5*, 345-359.
- (44) Winston, C. T.; Boger, D. L. Sequence-selective DNA recognition: natural products and nature’s lessons. *Chem. Bio.* **2004**, *11*, 1607-1617.
- (45) Hirayama, H.; Tamaoka, J.; Horikoshi, K. Improved immobilization of DNA to microwell plates for DNA-DNA hybridization. *Nucleic Acids Res.* **1996**, *24*, 4098-4099.
- (46) Yang, F.; Teves, S. S.; Kemp, C. J.; Henikoff, S. Doxorubicin, DNA torsion, and chromatin dynamics. *BBA-Rev Cancer* **2014**, *1845*, 84-89.
- (47) Bailly, C.; Chessari, G.; Carrasco, C.; Joubert, A.; Mann, J.; Wilson, W. D.; Neidle, S. Sequence-specific minor groove binding by bis-benzimidazoles: water molecules in ligand recognition. *Nucleic Acids Res.* **2003**, *31*, 1514-1524.
- (48) Bailly, C.; Chaires, J. B. Sequence-specific DNA minor groove binders. Design and synthesis of netropsin and distamycin analogues. *Bioconjugate Chem.* **1998**, *9*, 513-538.
- (49) Fornander, L. H.; Wu, L.; Billeter, M.; Lincoln, P.; Nordén, B. Minor-groove binding drugs: where is the second Hoechst 33258 molecule? *J. Phys. Chem. B* **2013**, *117*, 5820-5830.
- (50) Marky, L. A.; Breslauer, K. J. Origins of netropsin binding affinity and specificity: correlations of thermodynamic and structural data. *Proc. Natl. Acad. Sci. U. S. A.* **1987**, *84*, 4359-4363.
- (51) Zhou, Z.; Hu, Y.; Shan, X.; Li, W.; Bai, X.; Wang, P.; Lu, X. Revealing three stages of DNA-cisplatin reaction by a solid-state nanopore. *Sci. Rep.* **2015**, *5*, 11868.

- (52) Lam, K. S. New aspects of natural products in drug discovery. *Trends Microbiol.* **2007**, *15*, 279-289.
- (53) Garcia, D. E.; Baidoo, E. E.; Benke, P. I.; Pingitore, F.; Tang, Y. J.; Villa, S.; Keasling, J. D. Separation and mass spectrometry in microbial metabolomics. *Curr. Opin. Microbiol.* **2008**, *11*, 233-239.
- (54) Concepcion, J.; Witte, K.; Wartchow, C.; Choo, S.; Yao, D.; Persson, H.; Wei, J.; Li, P.; Heidecker, B.; Ma, W. Label-free detection of biomolecular interactions using BioLayer interferometry for kinetic characterization. *Comb. Chem. High Throughput Screen.* **2009**, *12*, 791-800.
- (55) Fox, K. R.; Wakelin, L. P.; Waring, M. J. Kinetics of the interaction between echinomycin and deoxyribonucleic acid. *Biochemistry* **1981**, *20*, 5768-5779.
- (56) Van Dyke, M. M.; Dervan, P. B. Echinomycin binding sites on DNA. *Science* **1984**, *225*, 1122-1127.
- (57) Barceló, F.; Capó, D.; Portugal, J. Thermodynamic characterization of the multivalent binding of chartreusin to DNA. *Nucleic Acids Res.* **2002**, *30*, 4567-4573.
- (58) Li, H.; Jiang, Z.; Zhang, R. Fluorescence quenching and the binding interaction of lumichrome with nucleic acids. *Chi. Sci. Bull.* **2010**, *55*, 2829-2834.
- (59) Eldridge, G. R.; Vervoort, H. C.; Lee, C. M.; Cremin, P. A.; Williams, C. T.; Hart, S. M.; Goering, M. G.; O'Neil-Johnso, M.; Zeng, L. High-throughput method for the production and analysis of large natural product libraries for drug discovery. *Anal. Chem.* **2002**, *74*, 3963-3971.